

Liver and brain mitochondria preparation

Mouse liver mitochondria were prepared as described and resuspended in MRM buffer (250 mM sucrose, 10 mM HEPES, pH 7.5, 1 mM ATP, 5 mM sodium succinate, 80 μ M ADP, 2 mM K_2HPO_4) at a concentration of 0.5 mg ml⁻¹ (ref. 18). Rat liver mitochondria were isolated from 4–6-month-old Fischer 344 \times brown Norway F₁ rats by differential centrifugation as described, except the final wash and resuspension buffer had no EGTA, EDTA or BSA²⁷. Non-synaptosomal rat brain mitochondria were prepared from forebrains of ~8-week Fischer 344 \times brown Norway rats (Ficoll gradient purification)^{28,29}.

In vitro cytochrome c release

An aliquot of 25 μ l of 0.5 mg ml⁻¹ mouse liver mitochondrial preparation was preincubated with minocycline or cyclosporin A for 5 min in MRM buffer. Mitochondria were incubated with 100 μ M CaCl₂ or 100 ng of purified mouse Bid protein¹⁷ at 30 °C for 30 min (CaCl₂) or for one hour (Bid). Mixtures were centrifuged at 10,000g at 4 °C for 10 min and the supernatant evaluated by western blot.

$\Delta\Psi$ /swelling measurements

Rat brain mitochondria (1 mg ml⁻¹ in 100 mM KCl, 75 mM mannitol, 25 mM sucrose, 10 mM Tris, 1 mM K-PO₄ (pH 7.3)) containing tetraphenyl phosphonium (TPP⁺), 25 μ M Ca²⁺ (from buffer and TPP⁺ stock) and minocycline (see key in Fig. 3d, e) were added at $t = 0$ and energized where marked (Fig. 3d, e) with 5 mM glutamate, 5 mM malate, 1 mM ATP and 80 μ M ADP. Bolus doses of 40 μ M Ca²⁺ were added where shown (Fig. 3d, e). Simultaneous measurement of $\Delta\Psi$ and light transmittance in stirred samples was accomplished using a four-channel respiration system designed by B. Krasnikov (ref. 30, and manuscript in preparation). Oxygen uptake, $\Delta\Psi$, and Ca²⁺ were measured using Clark, TPP⁺, and Ca²⁺-sensitive electrodes, respectively. A₆₆₀ was measured using a diode. Experiments were carried out in triplicate. Plots shown are representative. Mixtures were sampled and centrifuged at 10,000g at 4 °C for 10 min. Supernatants were evaluated for cytochrome c (Fig. 3c).

Rat liver mitochondria were used for minocycline-mitochondria co-titration. PT induction was assessed spectrophotometrically by suspending mitochondria at 25 °C in 200 μ l of 310 mM sucrose, 30 mM KCl, 3 mM K-HEPES (pH 7.3), with 5 μ M added Ca²⁺. Samples with 0.1 mg mitochondria per ml had 100 μ M K-PO₄; samples with 0.03 mg mitochondria per ml had 30 μ M K-PO₄. Changes in transmittance at 520 nm were followed for 30 min using a SpectraMax 250 Plate Reader (Molecular Dynamics). Minocycline does not display appreciable absorbance at this wavelength.

Light scattering data are qualitatively identical at the two wavelengths used. The lower wavelength (520 nm) was used on the plate reader because it gives a slightly better signal:noise profile. The higher wavelength (660 nm) was used in the four-channel system because the light-emitting diode can only be used at that wavelength.

Received 21 February; accepted 5 April 2002.

1. Yrjanheikki, J., Keinanen, R., Pellikka, M., Hokfelt, T. & Koistinaho, J. Tetracyclines inhibit microglial activation and are neuroprotective in global brain ischemia. *Proc. Natl Acad. Sci. USA* **95**, 15769–15774 (1998).
2. Chen, M. *et al.* Minocycline inhibits caspase-1 and caspase-3 expression and delays mortality in a transgenic mouse model of Huntington disease. *Nature Med.* **6**, 797–801 (2000).
3. Sanchez Mejia, R. O., Ona, V. O., Li, M. & Friedlander, R. M. Minocycline reduces traumatic brain injury-mediated caspase-1 activation, tissue damage, and neurological dysfunction. *Neurosurgery* **48**, 1393–1401 (2001).
4. Tikka, T., Fiebich, B. L., Goldsteins, G., Keinanen, R. & Koistinaho, J. Minocycline, a tetracycline derivative, is neuroprotective against excitotoxicity by inhibiting activation and proliferation of microglia. *J. Neurosci.* **21**, 2580–2588 (2001).
5. Wu, D. C. *et al.* Blockade of microglial activation is neuroprotective in the 1-methyl-4-phenyl-1,2,3,6-tetrahydropyridine mouse model of Parkinson disease. *J. Neurosci.* **22**, 1763–1771 (2002).
6. Du, Y. *et al.* Minocycline prevents nigrostriatal dopaminergic neurodegeneration in the MPTP model of Parkinson's disease. *Proc. Natl Acad. Sci. USA* **98**, 14669–14674 (2001).
7. Friedlander, R. M., Brown, R. H., Gagliardini, V., Wang, J. & Yuan, J. Inhibition of ICE slows ALS in mice. *Nature* **388**, 31 (1997).
8. Almer, G., Vukosavic, S., Romero, N. & Przedborski, S. Inducible nitric oxide synthase up-regulation in a transgenic mouse model of familial amyotrophic lateral sclerosis. *J. Neurochem.* **72**, 2415–2425 (1999).
9. Li, M. *et al.* Functional role of caspase-1 and caspase-3 in an ALS transgenic mouse model. *Science* **288**, 335–339 (2000).
10. Brogden, R. N., Speight, T. M. & Avery, G. S. Minocycline: A review of its antibacterial and pharmacokinetic properties and therapeutic use. *Drugs* **9**, 251–291 (1975).
11. Ona, V. O. *et al.* Inhibition of caspase-1 slows disease progression in a mouse model of Huntington's disease. *Nature* **399**, 263–267 (1999).
12. Rowland, L. P. & Schneider, N. A. Amyotrophic lateral sclerosis. *N. Engl. J. Med.* **344**, 1688–1700 (2001).
13. Rosen, D. R. *et al.* Mutations in Cu/Zn superoxide dismutase gene are associated with familial amyotrophic lateral sclerosis. *Nature* **362**, 59–62 (1993).
14. Gurney, M. E. *et al.* Motor neuron degeneration in mice that express a human Cu,Zn superoxide dismutase mutation. *Science* **264**, 1772–1775 (1994).
15. Wong, P. C. *et al.* An adverse property of a familial ALS-linked SOD1 mutation causes motor neuron disease characterized by vacuolar degeneration of mitochondria. *Neuron* **14**, 1105–1116 (1995).
16. Green, D. R. & Reed, J. C. Mitochondria and apoptosis. *Science* **281**, 1309–1312 (1998).
17. Li, H., Zhu, H., Xu, C. J. & Yuan, J. Cleavage of BID by caspase 8 mediates the mitochondrial damage in the Fas pathway of apoptosis. *Cell* **94**, 491–501 (1998).
18. Luo, X., Budihardjo, I., Zou, H., Slaughter, C. & Wang, X. Bid, a Bcl2 interacting protein, mediates cytochrome c release from mitochondria in response to activation of cell surface death receptors. *Cell* **94**, 481–490 (1998).
19. Zamzami, N. *et al.* Bid acts on the permeability transition pore complex to induce apoptosis. *Oncogene* **19**, 6342–6350 (2000).

20. Bernardi, P., Scorrano, L., Colonna, R., Petronilli, V. & Di Lisa, F. Mitochondria and cell death. Mechanistic aspects and methodological issues. *Eur. J. Biochem.* **264**, 687–701 (1999).
21. Kristal, B. S. & Dubinsky, J. M. Mitochondrial permeability transition in the central nervous system: induction by calcium cycling-dependent and -independent pathways. *J. Neurochem.* **69**, 524–538 (1997).
22. Friberg, H., Conner, C., Halestrap, A. P. & Wieloch, T. Differences in the activation of the mitochondrial permeability transition among brain regions in the rat correlate with selective vulnerability. *J. Neurochem.* **72**, 2488–2497 (1999).
23. Shimizu, S., Narita, M. & Tsujimoto, Y. Bcl-2 family proteins regulate the release of apoptogenic cytochrome c by the mitochondrial channel VDAC. *Nature* **399**, 483–487 (1999).
24. Guegan, C., Vila, M., Rosoklija, G., Hays, A. P. & Przedborski, S. Recruitment of the mitochondrial-dependent apoptotic pathway in amyotrophic lateral sclerosis. *J. Neurosci.* **21**, 6569–6576 (2001).
25. Hartley, D. M. *et al.* Protofibrillar intermediates of amyloid beta-protein induce acute electrophysiological changes and progressive neurotoxicity in cortical neurons. *J. Neurosci.* **19**, 8876–8884 (1999).
26. Friedlander, R. M. *et al.* Expression of a dominant negative mutant of interleukin-1 beta converting enzyme in transgenic mice prevents neuronal cell death induced by trophic factor withdrawal and ischemic brain injury. *J. Exp. Med.* **185**, 933–940 (1997).
27. Kristal, B. S. & Brown, A. M. Apoptogenic ganglioside GD3 directly induces the mitochondrial permeability transition. *J. Biol. Chem.* **274**, 23169–23175 (1999).
28. Lai, J. C. & Clark, J. B. Preparation of synaptic and nonsynaptic mitochondria from mammalian brain. *Methods Enzymol.* **55**, 51–60 (1979).
29. Kristal, B. S., Staats, P. N. & Shestopalov, A. I. Biochemical characterization of the mitochondrial permeability transition in isolated forebrain mitochondria. *Dev. Neurosci.* **22**, 376–383 (2000).
30. Krasnikov, B. F., Kuzmina, A. E. & Zorov, D. B. The Ca²⁺-induced pore opening in mitochondria energized by succinate-ferricyanide electron transport. *FEBS Lett.* **419**, 137–140 (1997).

Acknowledgements

We thank E. Friedlander for editorial assistance, B. Krasnikov for discussion concerning the 4-channel mitochondrial chamber, and M. Lukyanova for technical assistance. Mouse Bid expression construct was provided by H. Li and J. Yuan. This work was supported by Project A.L.S. (R.M.F., S.G., S.P.), the NIH (R.M.F., D.M.H., R.J.F., S.P., B.S.K.), the Huntington's Disease Society of America (R.M.F.), the Hereditary Disease Foundation (R.M.F., B.S.K.), the Muscular Dystrophy Association (R.M.F., S.P.), the Veterans Administration (R.J.F.), Hope for ALS (S.G.), Ride for ALS (S.G.), ALS Association (S.P.), the US Department of Defense (S.P.), the Lowenstein Foundation (S.P.), the Smart Foundation (S.P.), and the Parkinson's Disease Foundation (S.P.).

Competing interests statement

The authors declare that they have no competing financial interests.

Correspondence and requests for materials should be addressed to R.M.F. (e-mail: rfriedlander@rics.bwh.harvard.edu).

Extensive and divergent circadian gene expression in liver and heart

Kai-Florian Storch^{*}, Ovidiu Lipan[†], Igor Leykin[†], N. Viswanathan[‡], Fred C. Davis[‡], Wing H. Wong^{†§} & Charles J. Weitz^{*}

^{*} Department of Neurobiology, Harvard Medical School; [†] Department of Biostatistics, Harvard School of Public Health; and [‡] Department of Biology, Northeastern University, Boston, Massachusetts 02115, USA
[§] Department of Statistics, Harvard University, Cambridge, Massachusetts 02138, USA

Many mammalian peripheral tissues have circadian clocks^{1–4}; endogenous oscillators that generate transcriptional rhythms thought to be important for the daily timing of physiological processes^{5,6}. The extent of circadian gene regulation in peripheral tissues is unclear, and to what degree circadian regulation in different tissues involves common or specialized pathways is unknown. Here we report a comparative analysis of circadian gene expression *in vivo* in mouse liver and heart using oligonucleotide arrays representing 12,488 genes. We find that peripheral circadian gene regulation is extensive (≥ 8 –10% of the genes expressed in each tissue), that the distributions of circadian phases in the two tissues are markedly different, and that very

few genes show circadian regulation in both tissues. This specificity of circadian regulation cannot be accounted for by tissue-specific gene expression. Despite this divergence, the clock-regulated genes in liver and heart participate in overlapping, extremely diverse processes. A core set of 37 genes with similar circadian regulation in both tissues includes candidates for new clock genes and output genes, and it contains genes responsive to circulating factors with circadian or diurnal rhythms.

Mice were entrained (synchronized) to a 12-h light/dark cycle for ≥ 2 weeks, and then placed in constant dim light (less than 1 lx) for ≥ 42 h. We collected tissues at 4-h intervals over two circadian cycles (12 time points). RNA isolated from livers and hearts was analysed on oligonucleotide arrays^{7,8} representing 30–40% of the estimated total number of mouse genes^{9,10}.

We identified circadian patterns in the gene expression data by a series of filtering steps. For each gene we required: (1) a positive correlation between the first and second days (selects for a daily repetition); (2) a negative autocorrelation at 12 h (removes ultradian oscillations and noise); (3) an amplitude threshold (removes trivial oscillations); and (4) a threshold for the maximum signal (removes unreliable data). To optimize the filtering parameters, we designated nine 'guide genes' (*Per1*, *Per2*, *Per3*, *Bmal1* (also known as *Mop3*), *Tef*, *Dpb*, *E4bp4*, *Cry1* and *Cry2*) that are known to exhibit circadian regulation in both tissues. The guide genes provided a variety of phases, amplitudes and waveforms. We systematically varied the parameters to find combinations that minimized the overall number of genes selected but maximized the number of guide genes selected. We identified parameters that retained only about 4% of the genes on the array but $\geq 67\%$ of the guide genes. Further increasing the stringency resulted in sharp reductions in the selection of guide genes and other genes.

This procedure identified 575 genes in liver and 462 genes in heart with circadian expression patterns (Fig. 1). The oscillations showed a variety of phases, amplitudes and waveforms. To estimate the contribution of noise, we created control data sets identical in content to the experimental data set, by random permutation of time order and redistribution of amplitudes and means. Filtering 100 different control data sets for each tissue with the same parameters as above resulted in selection of 90 ± 9.2 (s.d.) genes for liver and 54 ± 7.8 genes for heart. Thus we estimate that 16% of our selected genes for liver and 12% for heart can be ascribed to noise. Of 51 genes regulated by a circadian clock recently identified in mouse liver by differential display¹¹, 15 were represented on the array, and none were guide genes. Of these, 8 were included in the liver circadian set. It seems likely that our analysis has identified a substantial fraction of clock-regulated genes but probably provides an underestimate.

Based on a probability of detection (see http://www.affymetrix.com/products/algorithms_tech.html for statistical algorithms for monitoring gene expression on GeneChip probe arrays) of $P < 0.05$ on at least 7 of the 12 arrays, we classified as expressed a total of 4,805 genes in liver and 5,120 in heart (a total of 3,953 genes in common). Given that 30–40% of all mouse genes are represented on the array, our estimates agree well with evidence that most cell types express 10,000–15,000 genes¹². After accounting for noise, we calculate that approximately 10% of the genes expressed in liver and about 8% of the genes expressed in heart show circadian regulation. Our data suggest a considerably greater prevalence of circadian regulation at low amplitudes, particularly in heart (data not shown). Although it is probable that the clock within each tissue drives most circadian gene regulation in the tissue, our *in vivo* analysis cannot distinguish genes driven locally from those driven by circadian signals generated in the suprachiasmatic nucleus¹³ or elsewhere. In a fibroblast cell line, a model for local circadian regulation, about 2% of the expressed genes were regulated by a circadian clock¹⁴, but this is probably a substantial underestimate¹⁴ because of damping of circadian oscillations¹.

The expression profiles of the circadian gene sets are displayed in Fig. 1. In liver (Fig. 1a), the oscillations showed a broad distribution of phases (Fig. 1b). In contrast, in heart (Fig. 1c) most of the genes showed synchronous peak expression at a circadian time of about 4 h (Fig. 1d, CT 4), a phase very sparsely represented in the liver set. This marked difference in circadian phase distribution was unaffected by significant relaxation or tightening of the filtering parameters. Thus, despite a similar number of genes with circadian expression in liver and heart, the timing of circadian gene regulation in the two tissues is markedly different, even though the molecular clocks in the two tissues were synchronized (Fig. 1b, d; phase markers).

The liver and heart circadian gene sets revealed very little overlap, with only 52 genes in common. Of these, a core set of only 37 showed essentially identical phases of peak expression in both

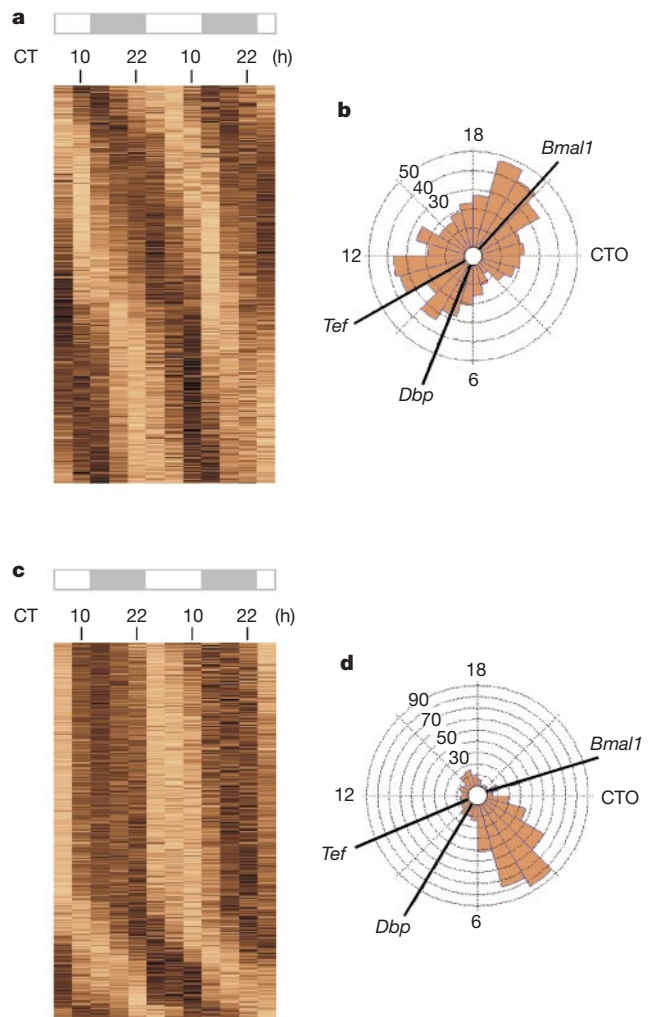


Figure 1 Temporal profiles of circadian gene expression in liver (**a, b**) and heart (**c, d**). **a, c**, Each column represents a circadian time point and each row a gene, with the genes ordered by the phase of maximal expression as determined by Fourier analysis. Light shades represent expression values above the mean for the gene; dark shades below the mean. Numbers at the top represent the circadian time (CT), and the bar represents the time of subjective day (white) and subjective night (grey). For a complete list of genes and associated expression values, see Supplementary Information. **b, d**, Phase histograms for genes with circadian expression patterns in liver and heart. Numbers on nested circles represent numbers of genes. CT0, circadian time zero hour. *Bmal1*, *Dpb* and *Tef* are genes with known robust circadian expression serving as phase markers for the circadian clock within each tissue.

tissues. This remarkable divergence in circadian gene regulation could simply reflect preferential regulation of tissue-specific genes by the clock in each tissue. We therefore examined the genes showing circadian expression only in liver or only in heart for detectable expression in the other. Of the 523 genes with circadian regulation only in liver, 316 (60%) were detectably expressed in heart. Conversely, of the 410 genes with circadian regulation only in heart, 242 (59%) were detectably expressed in liver. Thus circadian regulation of tissue-specific genes cannot account for the divergence of circadian gene regulation between liver and heart.

The divergence of liver and heart in the timing and content of circadian gene regulation suggests a specialized role of circadian clocks in each tissue, but the sheer extent of circadian gene regulation in both tissues implies a broad function. To address this apparent contradiction, we used the gene ontology representation¹⁵, which organizes biological knowledge into three hierarchies: biological process, molecular function and cellular component. Gene ontology provides a general and objective basis for analysing and comparing large biological data sets.

First we mapped the genes in our various sets onto the gene ontology hierarchies. Of the 4,805 genes expressed in liver and the 5,120 expressed in heart, 3,023 (63%) and 3,182 (62%), respectively, made a match to at least one gene ontology term; each term corresponds to a node (category) on a gene ontology hierarchy. Of the 575 genes in the liver circadian set and the 462 genes in the heart circadian set, 388 (67%) and 297 (64%), respectively, matched at least one gene ontology term, proportions similar to the expressed sets.

To create a framework for comparing the functions of liver and heart circadian gene regulation, we merged the set of genes expressed in liver with the set expressed in heart, and mapped the combined set onto the gene ontology hierarchy for biological process. The resulting map can be displayed as a tree that shows

only those nodes (biological process terms) represented by genes in the combined liver and heart expressed gene set. Figure 2 shows this tree at low resolution (grey structure with dots representing nodes). The most general processes are represented at the top (examples are marked by numbers); the most specialized processes are shown at the bottom. Onto this tree we superimposed the nodes making a match to at least one gene in the circadian set for liver (green dots) and those making a match to at least one gene in the circadian set for heart (red dots)—many make a match to both (yellow dots).

Several conclusions emerge from this global comparison. First, the circadian gene sets from both liver and heart map across the entire tree. Thus circadian clocks influence extremely diverse processes, even within a single tissue. Second, genes in the circadian sets for liver and heart map to many nodes in common, even at deep levels representing highly specialized processes. This result was robust across different filtering and mapping parameters. A few exceptions were evident, such as the cluster of nodes representing amino-acid metabolism (liver only; green arrow) and the cluster representing G-protein-coupled receptor signalling cascades (heart only; red arrow). We conclude that clock-regulated genes in liver and heart participate in many related or overlapping processes, even though the two sets of genes have almost no overlap in content or temporal expression pattern.

Our results, which address circadian gene regulation, provide a broad view of the probable physiological functions of peripheral clocks; however, some caveats apply. First, because protein rhythms depend in part on protein turnover, a transcript with a circadian rhythm does not necessarily code for a protein with a significant circadian rhythm; conversely, a transcript with an undetected low-amplitude circadian rhythm could code for a protein with a significant circadian rhythm. Second, a protein circadian rhythm might have little physiological consequence if, at its trough, the protein is not limiting or if it does not participate in a rate-limiting

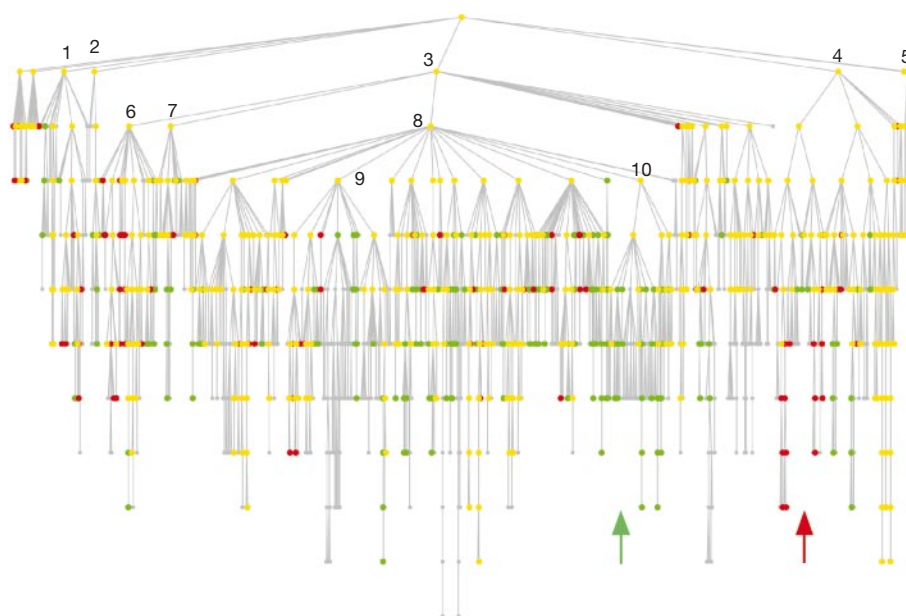


Figure 2 Global comparison of biological processes associated with the genes exhibiting circadian expression in liver and heart. The tree (grey dots and connecting paths) represents those categories (dots) in the gene ontology hierarchy for biological process that matched one or more genes expressed in liver or heart. Superimposed on the tree are the biological processes that matched one or more genes in the liver circadian set (green dots), the heart circadian set (red dots), or both (yellow dots). Marked are atypical examples of process clusters matching only to the circadian gene set from liver (green

arrow) or heart (red arrow). Selected examples of biological process categories are indicated by the following numbers: 1, developmental process; 2, death; 3, cell growth and/or maintenance; 4, cell communication; 5, behaviour; 6, transport; 7, stress response; 8, metabolism; 9, (metabolism) nucleobase/nucleoside/nucleotide; 10, (metabolism) amino-acid derivative. More than 1,400 biological process categories are shown.

process; conversely, a low-amplitude protein rhythm might drive a high-amplitude physiological rhythm if the protein participates in a cooperative process.

Because the set of genes with circadian regulation in both liver and heart is so small, it is likely to be highly enriched in genes important for the core functions of all peripheral clocks, such as synchronization to circulating factors, generation of rhythmicity, and control of transcriptional outputs. The expression profiles of the genes in the core common set are shown in Fig. 3a, arranged by the phase of peak expression as determined for liver. The slight disorder in the heart profiles arises from minor discrepancies between liver and heart in the phase assignments for some genes. The distribution of phases is essentially bimodal (Fig. 3b), with most genes showing peak expression between circadian time 6 h and 14 h, and a smaller group peaking in phase at about circadian time 20 h. Comparisons of temporal expression patterns for individual genes in liver and heart are shown in Fig. 4; in many cases the waveform is conserved in the two tissues.

Six of the nine guide genes appear in the common set (Fig. 4), but *Per3*, *Cry1* and *Cry2* do not because our filtering parameters excluded them from one or both circadian sets on the basis of low expression and/or amplitude. Also appearing (but not a guide gene) was the nuclear receptor gene *Rev-erb-α* (Fig. 4), which is known to be clock-regulated in different tissues¹⁶.

The other genes in the core common set were not previously known to exhibit circadian expression. *Zfp36* and *Sox3*, coding for transcription factors, are potential clock genes or core output genes, similar to *Dbp*¹⁷. Genes involved in chromatin regulation (*Chrac1*, *Rad23b* homologue, DNMT1-associated protein-1) and in ubiquitin pathways (*Usp2*, Fig. 4, and *Herpud1*) suggest a general circadian influence on gene expression and protein stability, respectively. The signal-transducing kinases *Gprk7* (Fig. 4) and *Stk23*, and the protein kinase-A regulatory subunit *Prkar1* are plausibly involved in entrainment, outputs, or regulation of circadian period, as known for other kinases¹⁸. *Pbef* (Fig. 4) and *Tnfaip2* code for secreted factors that are plausible transmitters of circadian information

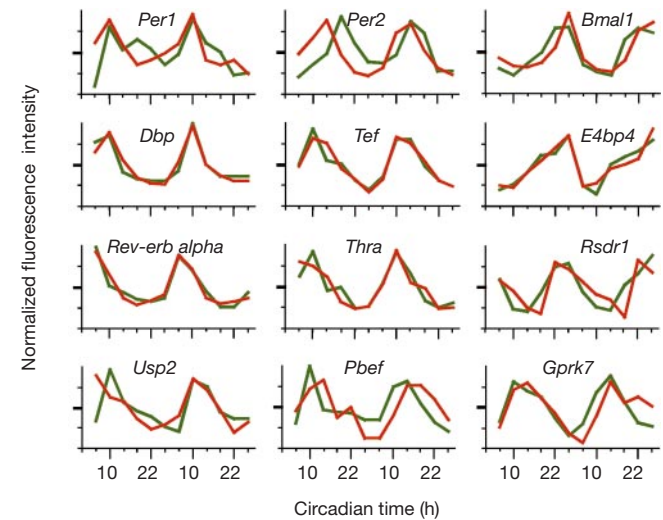


Figure 4 Individual circadian expression profiles of selected genes from the set common to liver and heart. Liver profiles are in green; heart profiles are in red. Gene symbols/names are indicated in Fig. 3.

within tissues or humorally to distant sites.

Five genes in the common set are regulated by factors with a diurnal or circadian rhythm in the circulation, of which glucocorticoids³ and retinoids⁴ have been proposed to act as entrainment signals for peripheral clocks. The gene *Thra* (Fig. 4), coding for the thyroid hormone receptor- α , is itself induced by the thyroid hormones T3 and T4 (ref. 19), and the phase of its rhythmic expression agrees with the humoral circadian rhythm of T3 and T4 in rat²⁰. Transcription of *Rev-erb- α* is inhibited by glucocorticoids¹⁶, and the timing of the decline in its expression agrees well

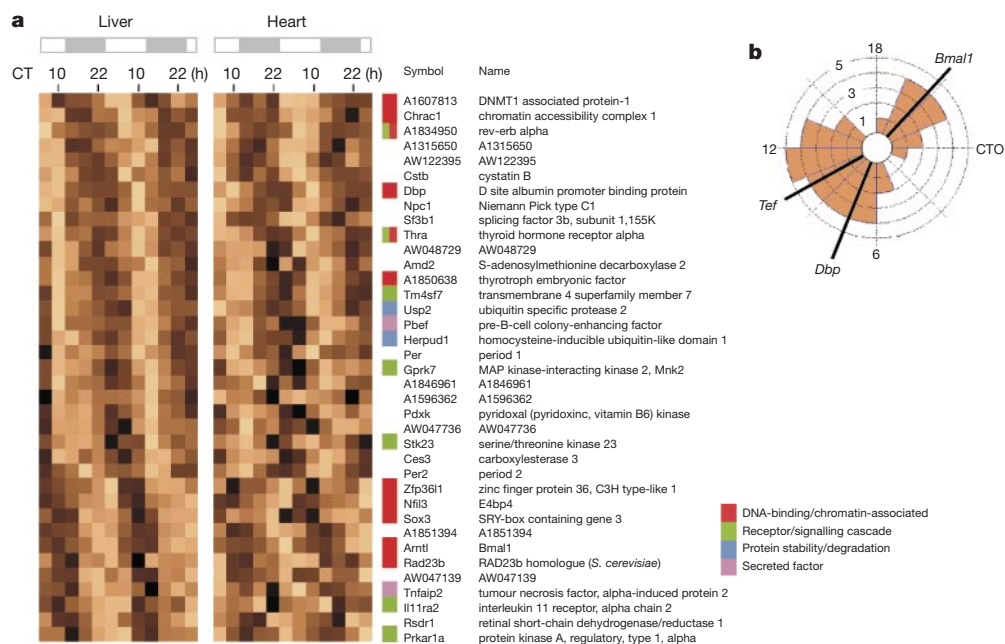


Figure 3 Temporal expression profiles of genes showing circadian regulation in both liver and heart. **a**, Profiles as in Fig. 1, ordered by phase as determined for liver. Annotation for selected genes is indicated by the colour code in the key; gene symbols and names are

from LocusLink. Uncharacterized genes are designated by GenBank accession numbers. **b**, Phase histogram of gene expression profiles in **a**; as in Fig. 1.

with the rising phase of the cortisol rhythm in mice²¹. The gene *RsdR* (Fig. 4) is induced by retinoids²², and *Tnfai2*²³ and *Zfp36*²⁴ are induced by tumour necrosis factor- α (TNF- α), both of which circulate with a diurnal rhythm^{25,26}. As transcriptional regulators, *Thra*, *Rev-erb-a* and *Zfp36* are plausible mediators of entrainment to humoral circadian signals, respectively thyroid hormones, glucocorticoids, and TNF- α .

Our work addresses global aspects of circadian gene regulation in mammals. We show that *in vivo* circadian gene regulation within individual tissues is extensive and diverse, broadly similar to circadian gene regulation in whole *Arabidopsis* plants²⁷ and *Drosophila* heads^{28,29}. Our comparative analysis of circadian gene expression in liver and heart reveals unsuspected features of circadian organization in peripheral tissues. Although the extent of circadian gene regulation in the two tissues is similar and the molecular clocks within the two tissues are in phase, liver and heart show little overlap in the timing and content of circadian gene regulation. Nevertheless, a global analysis of function suggests that circadian gene expression impinges on a large set of related and overlapping processes in the two tissues. These results suggest that a common core clock mechanism regulates similar, extremely diverse physiological processes in liver and heart, but that different downstream signalling circuits and effector genes carry out this regulation in the two tissues.

Note added in proof: A similar comparative analysis of circadian gene expression in the liver and suprachiasmatic nucleus has been reported³⁰. □

Methods

Animals, tissue collection and microarray hybridization

Mice (C57/Bl6; Charles River Laboratories) were killed by decapitation under dim white light (less than 1 lx), and livers and hearts were removed, immediately frozen in liquid nitrogen, and stored at -70°C . Total RNA was extracted from individual tissues using Trizol (Life Technologies) and selected for poly(A)⁺ RNA by one round of oligo-deoxythymidine selection (Oligotex, Qiagen). For each time point, 5 μg of poly(A)⁺ RNA or, in a few cases, 10 μg of total RNA from tissue from a single mouse was used to make biotin-labelled complementary RNA (cRNA), which was hybridized on an Affymetrix U74Av2 oligonucleotide array. cRNA generated from poly(A)⁺ RNA and total RNA performed equivalently. We carried out cRNA synthesis, hybridization and array scanning according to the Affymetrix GeneChip Expression Analysis Technical Manual. For identifying and annotating genes represented on the array, GenBank accession numbers were used to search UniGene and LocusLink databases.

Data analysis

Raw scanner image files were analysed with dChip⁸. For each gene, the dChip outputs ('raw expression values') for the first six time points (day 1) and the second six time points (day 2) were each set to a mean of 1 and a standard deviation of 0. We treated them separately because day 1 and day 2 samples were processed and hybridized to arrays separately. For each gene, the two normalized (n) data sets were then concatenated to obtain a 12-time-point expression profile (nday 1–nday 2).

Four parameters (P) were used to select for circadian expression patterns: (P1), autocorrelation of the concatenated 12 time points (nday 1–nday 2 versus nday 1–nday 2); (P2), correlation of each day with the other (nday 1–nday 1 versus nday 2–nday 2); (P3), a threshold for the maximum raw expression value within each day; and (P4), a threshold within each day for the variation of the raw expression value (determined from the standard deviation) divided by the mean raw expression value.

To optimize the parameters for selection of circadian expression patterns, we designated nine guide genes with documented circadian expression in both liver and heart (see text). Parameter selection was performed by moving along the coordinates of the four-dimensional parameter space, simultaneously minimizing the total number of genes selected while maximizing the number of guide genes selected. For estimation of noise within the selected data sets, we randomly permuted the 12 time points (nday 1–nday 2) and then assigned each gene an amplitude and a mean, randomly selected from the genes on the array. This procedure keeps the content of the data set constant while permuting the features operated on by each of the selection parameters. For a full account of the filtering procedures, see Supplementary Information.

Gene ontology maps

The comparative analysis of expression data using the Gene Ontology structured vocabulary was performed using the GoSurfer analysis tool, which will be described elsewhere (O.L. & K-F.S. *et al.*, manuscript in preparation). Briefly, GoSurfer creates unique identifiers for every path in a gene ontology graph and implements statistical and other tools for analysing path properties and relationships. The node coordinates of the tree displayed in Fig. 2 were created as follows. First, we extracted gene ontology identifiers associated with the genes in each of the sets or their human orthologues from LocusLink

(www.ncbi.nlm.nih.gov/LocusLink) or GO Annotations at the European Bioinformatics Institute (EBI) (<http://www.ebi.ac.uk>). Next we matched these gene ontology identifiers with the gene ontology for biological process (<http://www.geneontology.org>), and transformed this subset of the ontology into a tree structure, where each node represents a gene ontology identifier and where the branches indicate their hierarchical relationship as defined by the gene ontology. For the graphical presentation we used an existing Matlab program (Trimtreelayout) to generate the tree backbone.

Received 28 February; accepted 2 April 2002.

Published online 21 April 2002, DOI 10.1038/nature744.

- Balsalobre, A., Damiola, F. & Schibler, U. A serum shock induces circadian gene expression in mammalian tissue culture cells. *Cell* **93**, 929–937 (1998).
- Yamazaki, S. *et al.* Resetting central and peripheral circadian oscillators in transgenic rats. *Science* **288**, 682–685 (2000).
- Balsalobre, A. *et al.* Resetting of circadian time in peripheral tissues by glucocorticoid signaling. *Science* **289**, 2344–2347 (2000).
- McNamara, P. *et al.* Regulation of CLOCK and MOP4 by nuclear hormone receptors in the vasculature: a humoral mechanism to reset a peripheral clock. *Cell* **105**, 877–889 (2001).
- Reppert, S. M. & Weaver, D. R. Molecular analysis of mammalian circadian rhythms. *Annu. Rev. Physiol.* **63**, 647–676 (2001).
- Ripperger, J. A. & Schibler, U. Circadian regulation of gene expression in animals. *Curr. Opin. Cell Biol.* **13**, 357–362 (2001).
- Lockhart, D. J. *et al.* Expression monitoring by hybridization to high-density oligonucleotide arrays. *Nature Biotechnol.* **14**, 1675–1680 (1996).
- Li, C. & Wong, W. H. Model-based analysis of oligonucleotide arrays: expression index computation and outlier detection. *Proc. Natl Acad. Sci. USA* **98**, 31–36 (2001).
- Claverie, J.-M. Gene number: what if there are only 30,000 human genes? *Science* **291**, 1255–1257 (2001).
- Murphy, W. J., Stanyon, R. & O'Brien, S. J. Evolution of mammalian genome organization inferred from comparative gene mapping. *Genome Biol. (Review)* **2**, 0005.1–0005.8 (2001).
- Korrmann, B., Preitner, N., Rifat, D., Fleury-Olela, F. & Schibler, U. Analysis of circadian liver gene expression by ADDER, a highly sensitive method for the display of differentially expressed mRNAs. *Nucleic Acids Res.* **29**, E51 (2001).
- Velculescu, V. E. *et al.* Analysis of human transcriptomes. *Nature Genet.* **23**, 387–388 (1999).
- Klein, D. C., Moore, R. Y. & Reppert, S. M. (eds) *Suprachiasmatic Nucleus: The Mind's Clock* (Oxford Univ. Press, New York, 1991).
- Grundschober, C. *et al.* Circadian regulation of diverse gene products revealed by mRNA expression profiling of synchronized fibroblasts. *J. Biol. Chem.* **276**, 46751–46758 (2001).
- Ashburner, M. *et al.* Gene ontology: tool for the unification of biology. The Gene Ontology Consortium. *Nature Genet.* **25**, 25–29 (2000).
- Torra, I. P. *et al.* Circadian and glucocorticoid regulation of Rev-erb- α expression in liver. *Endocrinology* **141**, 3799–3806 (2000).
- Ripperger, J. A., Shearman, L. P., Reppert, S. M. & Schibler, U. CLOCK, an essential pacemaker component, controls expression of the circadian transcription factor DBP. *Genes Dev.* **14**, 679–689 (2000).
- Young, M. W. & Kay, S. A. Time zones: a comparative genetics of circadian clocks. *Nature Rev. Genet.* **2**, 702–715 (2001).
- Tata, J. R., Baker, B. S., Machuca, I., Rabelo, E. M. & Yamauchi, K. Autoinduction of nuclear receptor genes and its significance. *J. Steroid Biochem. Mol. Biol.* **46**, 105–119 (1993).
- Kalsbeek, A., Fliers, E., Franke, A. N., Wortel, J. & Buijs, R. M. Functional connections between the suprachiasmatic nucleus and the thyroid gland as revealed by lesioning and viral tracing techniques in the rat. *Endocrinology* **141**, 3832–3841 (2000).
- Harris, H. J., Kotelevtsev, Y., Mullins, J. J., Seckl, J. R. & Holmes, M. C. Intracellular regeneration of glucocorticoids by 11 β -hydroxysteroid dehydrogenase (11 β -HSD)-1 plays a key role in regulation of the hypothalamic-pituitary-adrenal axis: analysis of 11 β -HSD-1-deficient mice. *Endocrinology* **142**, 114–120 (2001).
- Chen, J., Maltby, K. M. & Miano, J. M. A novel retinoid-response gene set in vascular smooth muscle cells. *Biochem. Biophys. Res. Commun.* **281**, 475–482 (2001).
- Wolf, F. W. *et al.* B94, a primary response gene inducible by tumour necrosis factor- α , is expressed in developing hematopoietic tissues and the sperm acrosome. *J. Biol. Chem.* **269**, 3633–3640 (1994).
- Cooper, P., Potter, S., Mueck, B., Yousefi, S. & Jarai, G. Identification of genes induced by inflammatory cytokines in airway epithelium. *Am. J. Physiol. Lung Cell. Mol. Physiol.* **280**, L841–L852 (2001).
- Buchan, P. *et al.* Repeated topical administration of all-trans-retinoic acid and plasma levels of retinoic acids in humans. *J. Am. Acad. Dermatol.* **30**, 428–434 (1994).
- Petrovsky, N. & Harrison, L. C. The chronobiology of human cytokine production. *Int. Rev. Immunol.* **16**, 635–649 (1998).
- Harmer, S. L. *et al.* Orchestrated transcription of key pathways in *Arabidopsis* by the circadian clock. *Science* **290**, 2110–2113 (2000).
- Claridge-Chang, A. *et al.* Circadian regulation of gene expression systems in the *Drosophila* head. *Neuron* **32**, 657–671 (2001).
- McDonald, M. J. & Rosbash, M. Microarray analysis and organization of circadian gene expression in *Drosophila*. *Cell* **107**, 567–578 (2001).
- Panda, S. J. *et al.* Coordinated transcription of key pathways in the mouse by the circadian clock. *Cell* [online 2 April 2001] 10.1016/S0092867402007225 (2002).

Supplementary Information accompanies the paper on Nature's website (<http://www.nature.com>).

Acknowledgements

This work was supported by the Edward R. and Anne G. Lefler Center, Harvard Medical School and the National Eye Institute (C.J.W.), a Deutsche Forschungsgemeinschaft Postdoctoral Fellowship (K-F.S.), the National Institute of Child Health and Human

Development (F.C.D. and N.V.), and the National Human Genome Research Institute (W.H.W.). We thank S. Meng and the Harvard Center for Genomics Research for technical assistance and M.-C. Kao for programming.

Competing interests statement

The authors declare that they have no competing financial interests.

Correspondence and requests for materials should be addressed to C.J.W. (e-mail: cweitz@hms.harvard.edu).

Glutamate-receptor-interacting protein GRIP1 directly steers kinesin to dendrites

Mitsutoshi Setou*, Dae-Hyung Seog*†, Yosuke Tanaka*, Yoshimitsu Kanai*, Yosuke Takei*, Masahiko Kawagishi* & Nobutaka Hirokawa*

* Department of Cell Biology and Anatomy, Graduate School of Medicine, University of Tokyo, Hongo 7-3-1, Bunkyo-ku, Tokyo 113-0033, Japan
 † Department of Microbiology, College of Medicine, Inje University, Jingu, Busan 633-165, Korea

In cells, molecular motors operate in polarized sorting of molecules, although the steering mechanisms of motors remain elusive¹. In neurons, the kinesin motor² conducts vesicular transport such as the transport of synaptic vesicle components to axons³ and of neurotransmitter receptors to dendrites⁴, indicating that vesicles may have to drive the motor for the direction to be correct. Here we show that an AMPA (α -amino-3-hydroxy-5-methylisoxazole-4-propionate) receptor subunit—GluR2-interacting protein (GRIP1)—can directly interact and steer kinesin heavy chains to dendrites as a motor for AMPA receptors. As would be expected if this complex is functional, both gene targeting and dominant negative experiments of heavy chains of mouse kinesin showed abnormal localization of GRIP1. Moreover, expression of the kinesin-binding domain of GRIP1 resulted in accumulation of the endogenous kinesin predominantly in the somatodendritic area. This pattern was different from that generated by the overexpression of the kinesin-binding scaffold protein JSAP1 (JNK/SAPK-associated protein-1, also known as Mapk8ip3), which occurred predominantly in the somatoaxon area. These results indicate that directly binding proteins can determine the traffic direction of a motor protein.

The neuron, a good model of a polarized cell, is divided into two molecularly and functionally distinct domains: axons and dendrites. The precise targeting and localization of proteins within these domains are critical to every aspect of neuronal function^{1,5}. In neurons, conventional kinesin, which consists of two heavy chains (KHC: KIF5) and two light chains (KLC)^{1,2}, is a multifunctional transporter of both axonal cargo such as synapsin and GAP43 (ref. 3) and dendritic cargo such as messenger RNA⁶ and the AMPA receptor⁴ (Fig. 1a). To elucidate the mechanisms possibly regulating how kinesin moves toward axons and/or dendrites, we screened the binding regulators of kinesin in a yeast two-hybrid system⁷. By this screening, we identified the glutamate-receptor-interacting protein GRIP1 (refs 8, 9) as the strongest partner of a cargo-binding domain^{10,11} of kinesin heavy chain, and we further showed that binding proteins could regulate the polarity of kinesin traffic direction.

All KIF5 isozymes (KIF5A, KIF5B and KIF5C) contained the

minimal GRIP1-binding site (Fig. 1b). The binding site overlapped with the cargo-binding domain of the fungus kinesin, which lacks the light chains¹¹. The tails of other major neuronal KIFs, such as KIF1A, KIF1B β and KIF17 (which bound to the mLin10 PDZ domain in this assay⁷), did not bind to GRIP1. The affinity of direct KIF5–GRIP1 interaction *in vitro* by surface plasmon resonance analysis⁷ ($K_d = 1.9 \times 10^{-8}$ M) was in good agreement with that previously reported for kinesin tail binding to brain microsomes *in vitro*¹⁰. Therefore, we suggest that heavy chains of kinesin directly bind to GRIP1.

We next investigated whether kinesin transports GRIP1. We used ‘kinesin-null’ primary cultured extra-embryonic cells from KIF5b-

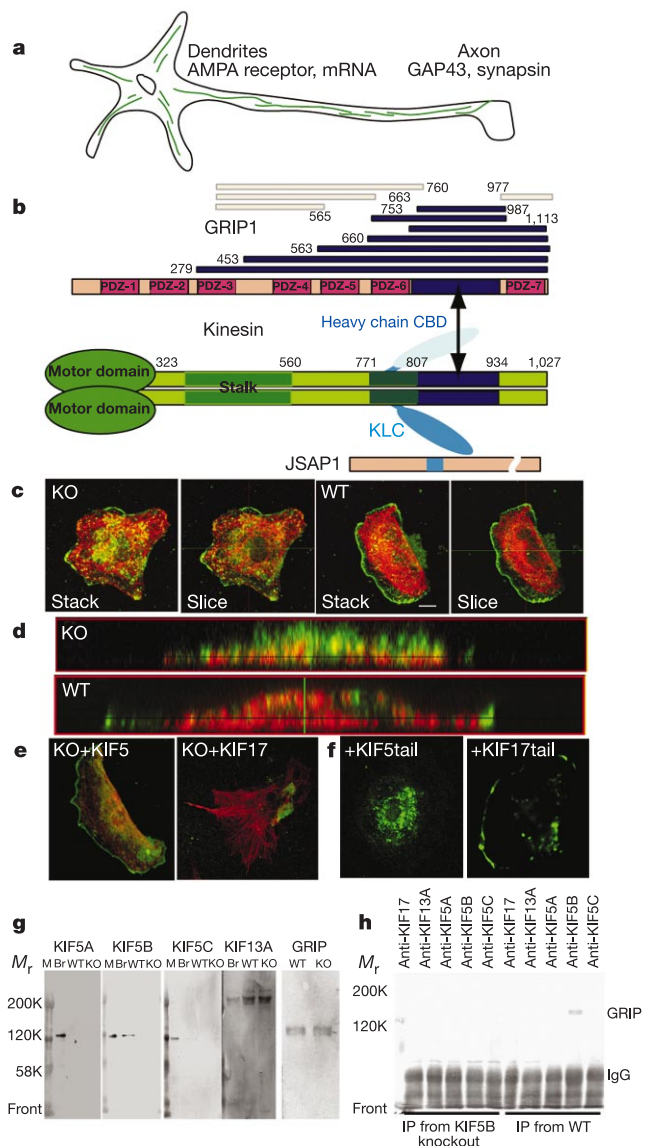


Figure 1 Kinesin binds to GRIP1, and is necessary for normal localization of GRIP1. **a**, Schematic diagram of a neuron and its reported kinesin cargo. **b**, Arrangement of GRIP1 and the kinesin binding domain. Blue boxes are the binding areas, with corresponding amino-acid positions indicated. Pale yellow boxes are areas of no binding. **c**, Aberrant localization of GRIP1 in cells lacking KIF5 (knockout cells, KO), wild type. GRIP1 is green; microtubules are red. Slices are confocal plane images at one-third of cell height. Scale bar, 20 μ m. **d**, The x - z sections of the cells in **c**. **e**, KIF5, but not KIF17, rescued KIF5-knockout cells. **f**, KIF5 tail, but not KIF17 tail, disturbed the localization of GRIP1. **g**, KIFs and GRIP1 expression level in knockout and wild-type cells. **h**, GRIP1 binds KIF5B in these cells. IP, immunoprecipitate. M, molecular mass marker; Br, brain.